Epitaxial ZnS, ZnSe and ZnS-ZnSe Superlattices Grown on (001)GaAs By Pulsed-Laser Ablation

J. W. McCamy,* Douglas H. Lowndes,† J. D. Budai,† G. E. Jellison, Jr.,† I. P. Herman,‡ and S. Kim‡
* Department of Materials Science and Engineering, The University of Tennessee, Knoxville, TN 37996-1200
† Solid State Division, Oak Ridge National Laboratory, Oak Ridge, TN 37831-6056
‡Department of Applied Physics, Columbia University, New York, NY 10027

Pulsed KrF (248nm) laser ablation of polycrystalline ZnS and ZnSe targets has been used to grow high quality, fully epitaxial ZnS and ZnSe thin films on (001) GaAs. Photoluminescence measurements of the ZnS thin films show strong edge emission, while ZnSe thin films show free excitonic as well as donor and acceptor peaks. By alternately ablating each target, strained layer superlattices of the form $(ZnSe)_m$-$(ZnS)_n$ were grown with as many as 65 periods of compositional modulation. A ZnS_xSe_{1-x} structure also was fabricated which simultaneously incorporated both continuously graded and abrupt compositional changes.

INTRODUCTION

Zinc sulfide (ZnS) and zinc selenide (ZnSe) are attractive thin-film optoelectronic materials because of their wide direct bandgaps (E_g = 3.7 eV and 2.7 eV, respectively). Potential applications for these materials include optically bistable switching devices for information processing [1,2], optical waveguides [3,4], and blue LEDs or laser diodes [5,6]. The two techniques most often used to grow ZnS, ZnSe and ZnS_xSe_{1-x} thin films and superlattices are metalorganic chemical vapor deposition (MOCVD) and molecular beam epitaxy (MBE). However, pulsed-laser ablation (PLA) has several practical advantages. These include stoichiometric transport of material from the ablation target to the substrate surface, when the laser beam conditions are correctly adjusted; growth of smooth films when the laser energy density, E_ρ, and the target surface morphology are controlled properly [13]; and, the ability to grade compositionally an epitaxial layer [7]. As with MBE, PLA films can be grown with submonolayer precision. Additionally, the composition of a PLA film is readily changed simply by exchanging solid ablation targets; consequently, strained layer superlattices of two or more materials are easily grown by PLA [8].

We recently showed that PLA is an attractive method for growth of uniform, fully epitaxial (e.g., in-plane-aligned) ZnS and ZnSe thin films and superlattices on (001) GaAs [9,10]. High resolution TEM (HRTEM), x-ray diffraction (XRD), and Rutherford backscattering spectrometry (RBS) showed that ZnS and ZnSe thin films grown by PLA are structurally comprable to those grown by MOCVD or MBE. However, it is not sufficient that PLA films simply be structurally 'good', in order for PLA to be considered competitive with other growth techniques, for the applications noted above. Additional requirements are imposed on the optical and electrical properties of the films. Finally, the quality of PLA strained-layer superlattices must be investigated, and a capability to compositionally grade multilayers and superlattices must be demonstrated. In this letter we present partial results of an ongoing effort to fully address these topics.

Mat. Res. Soc. Symp. Proc. Vol. 285. ©1993 Materials Research Society

EXPERIMENTAL

GaAs (001) substrates were degreased in organic solvents, then etched (15 s) in concentrated H_2SO_4. The substrate surfaces then were passivated in an $(NH_4)_2S_x$ solution, mounted on the substrate heater, and introduced into the growth chamber (2×10^{-7} Torr base pressure). Immediately before film growth, the substrates were heated to 420°C for 3 minutes, then cooled to the growth temperature. In previous work it was determined that the optimum temperature for PLA growth of ZnS on GaAs is 325°C, while for ZnSe the optimal growth temperature is 300°C [10]. Thus, in this work we maintained T_g = 325°C for growth of ZnS thin films and T_g = 300°C for ZnSe growth. For the Se-rich multilayers reported here we used T_g = 300°C; otherwise, T_g = 325°C was used.

A pulsed KrF (248nm) excimer laser beam (~35 ns FWHM pulse duration) was passed through an aperture and brought to a vertical focus on a 2.54 cm-diam polycrystalline ZnS or ZnSe target (Ångstrom Sciences, 99.999+ % purity) using a single +50 cm cylindrical lens. The data reported here were obtained using E_ℓ = 0.35 J/cm^2 and a target-substrate separation of 10.8 cm. The chamber was equipped with a multitarget holder that allows in situ target exchange, so that thin-film multilayers and superlattices could be grown simply by alternating targets. The film-growth rate was monitored in situ from interference oscillations in the intensity of a HeNe (633 nm) laser beam reflected from the upper and lower surfaces of the growing film. For the growth conditions given here, typical growth rates were ~0.2 nm per laser pulse for growth along the (001) direction.

RESULTS AND DISCUSSION

Multilayers and Superlattices

The exciton oscillator strength can be enhanced by quasi-two-dimensional confinement in a quantum well [11]. To determine if high quality Zn-based superlattices can be fabricated using PLA, structures of the form $(ZnSe)_m$-$(ZnS)_n$ were grown with as many as 65 periods of compositional modulation. Figure 1 shows the θ–2θ XRD pattern for a 65–period $(ZnSe)_6$-$(ZnS)_3$ superlattice grown on a 370 nm–thick ZnSe buffer layer. The growth rate (measured in situ) was 0.167 nm per shot. Thus, to achieve a period of 5 nm the ZnSe target was ablated for 20 shots followed by 10 shots on the ZnS target. Superlattice satellite peaks are easily seen in Fig. 1; their separation corresponds to a compositional modulation period of 4.8 nm, which compares well with the desired value. The expected lattice constant parallel to the surface normal for a superlattice with this structure is 0.556 nm (2θ = 67.3°), in good agreement with the zeroth peak assignment (2θ = 67.54°). The other peak assignments shown in Fig. 1 were made by approximating the superlattice as a $(ZnSe)_6$-$(ZnS)_3$ structure and calculating the diffraction peak positions using kinematical XRD theory. The presence of several orders of satellite peaks (Fig. 1) indicates that this $(ZnSe)_6$-$(ZnS)_3$ superlattice structure has sharp compositional interfaces, and is structurally comparable to superlattices of other materials grown by PLA and to superlattices grown by other techniques [8,12].

Compositionally Modulated Structures

It is expected that novel devices can be constructed by bandgap engineering (e.g., by continuously grading or abruptly modulating the semiconducting energy bandgap). By controlling the Cd content, Cheung [7] was able to spatially modify (in the growth direction) the position of the conduction band edge of PLA–grown

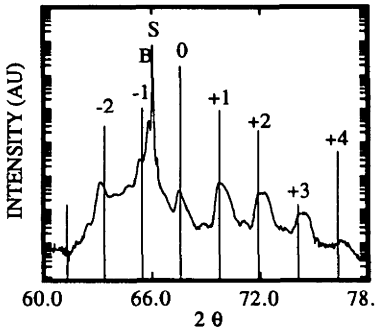

Figure 1. X-ray diffraction peaks for a 65–period ~ $(ZnS)_3$-$(ZnSe)_6$ strained–layer superlattice grown by PLA.

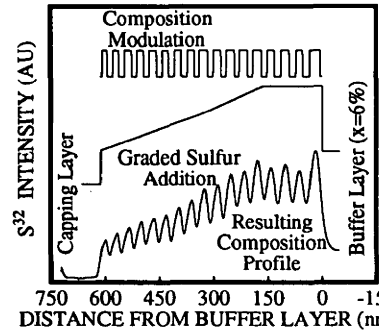

Figure 2. S^{32} profile measured by SIMS for a compositionally graded and modulated ZnS_xSe_{1-x} thin–film structure grown by PLA.

$Hg_{1-x}Cd_xTe$. In a similar manner, by controlling the sulfur content in ZnS_xSe_{1-x}, the position of the valence bandedge can be modified. Since sulfur addition decreases the lattice parameter, this technique also can be used to control strain in the film.

Figure 2 shows the sulfur compositional profile of a ZnS_xSe_{1-x} multilayered structure that was fabricated so as to simultaneously incorporate both continuously graded and abrupt compositional changes. The top two curves of Fig. 2 show separately the idealized graded and modulated profiles. The lower curve shows the resulting experimental sulfur profile, as determined by secondary ion mass spectroscopy (SIMS). For the graded profile (middle curve, Fig. 2) the sulfur content was held constant at 18% from 0 nm to 165 nm (measured from the top of the x = 6% buffer layer), and then decreased from 18% at 165 nm to 6% at 600 nm. The compositional modulation (top curve, Fig. 2) consisted of 16 1/2 periods of 36 nm each, within which the sulfur content was varied by ± 3%.

Optical Properties

The optical properties of thin (150–800 nm) ZnS and ZnSe films grown by PLA were investigated in the 1.5–5.3 eV region using spectroscopic two-channel polarization modulation ellipsometry [13]. To determine a film's dielectric function by this method it is necessary first to specify its layer–structure. A three-layer model was used, consisting of the GaAs substrate, the film, and a roughened film–surface layer. The thickness of the film and surface layer were determined using a single-term Lorentz approximation for the optical functions below the bandedge [14]. Once the thickness of each layer was determined, the dielectric function was determined accurately across the full spectral range. The dielectric function spectra for a thin film grown by PLA are shown in Figure 3, and for ZnS in Fig. 4. It can be seen that for both films, ε_2 approaches zero below the bandedge, while spectral features are seen clearly just above the bandedge. The transparency ($\varepsilon_2 \sim 0$) of these films below the bandedge indicates that they are of high optical quality, probably well suited for use as waveguides.

For the zincblende structure of ZnS and ZnSe, the fundamental optical absorption edge corresponds to a direct transition at the Γ–point in reciprocal space. Splitting of the valence band occurs by spin-orbit interaction, with the

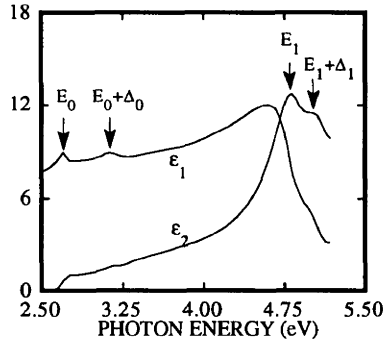

Figure 3. Real and imaginary parts of the dielectric function for a 800 nm-thick ZnS film grown by PLA.

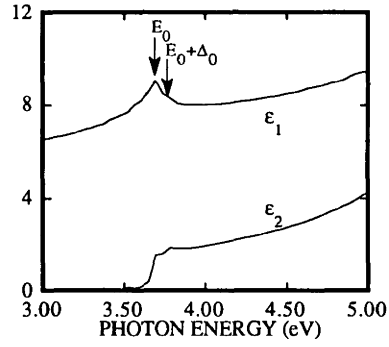

Figure 4. Real and imaginary parts of the dielectric function for a 250 nm-thick ZnSe film grown by PLA.

splitting energy represented by Δ_0. Table 1 shows optical transitions in the photon energy range from 1.5 eV to 5.3 eV. Also shown in the table are the corresponding transition energies for ZnS and ZnSe films grown by PLA. As can be seen, there is excellent agreement with previously published values, giving a further indication of the optical quality of the PLA films.

Table 1. Optical transitions and energies for ZnS and ZnSe. Published results are shown for comparison enclosed by ( ), with reference numbers indicated by [ ].

	E_0 (eV) $(\Gamma_8^v \rightarrow \Gamma_6^c)$	$E_0+\Delta_0$ (eV) $(\Gamma_7^v \rightarrow \Gamma_6^c)$	E_1 (eV) $(L_{4,5}^v \rightarrow L_6^c)$	$E_1+\Delta_1$ (eV) $(L_6^v \rightarrow L_6^c)$
ZnS	3.68 (3.68 [15])	3.76(3.75 [16])	(> 5.5 [17])	(> 5.5 [17])
ZnSe	2.68 (2.68[18])	3.13 (3.10 [18])	4.80 (4.75 [18])	5.03 (5.05 [18])

Photoluminescence Spectra

Photoluminescence spectra obtained at T = 9 K for an undoped 800 nm-thick ZnS film and for an undoped 230 nm-thick ZnSe film are shown in Figs. 5 and 6, respectively. Strong, near-bandedge peaks are seen for both materials. For the ZnS film, the I_{x1} peak is attributed to a neutral-donor bound-exciton, the I_{x2} and I_{x3} peaks are attributed to excitons bound to donor centers (possible Zn vacancies), and the I_{x3} peak to an acceptor bound-exciton. For the ZnSe film, the I_x peak is attributed to a neutral-donor bound-exciton, while the I_1^d peak is attributed to a deep-acceptor bound-exciton. The presence of both the I_x (2.798 eV) and the donor-acceptor-pair (DAP, 2.715 eV) emissions match the PL spectra of Ga-doped films [19]. Trace impurity analysis of the ZnSe PLA target revealed < 0.03 ppm Ga (the resolution limit). Thus, if the DAP emission is due to Ga, it most likely is due to Ga diffusing in from the GaAs substrate. Both light- and heavy-hole free excitions (X_{lh}, X_{hh}) are present in the ZnSe spectra. The X_{lh} feature is found on the high-energy of X_{hh} because of the compressive strain.

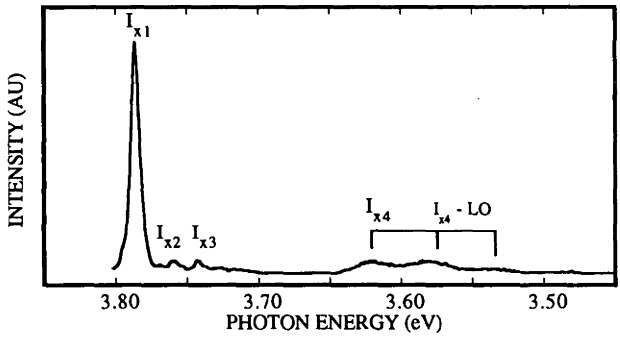

Figure 5. Photoluminescence spectrum at T = 9 K for an undoped 800 nm-thick ZnS film grown on (001) GaAs by PLA.

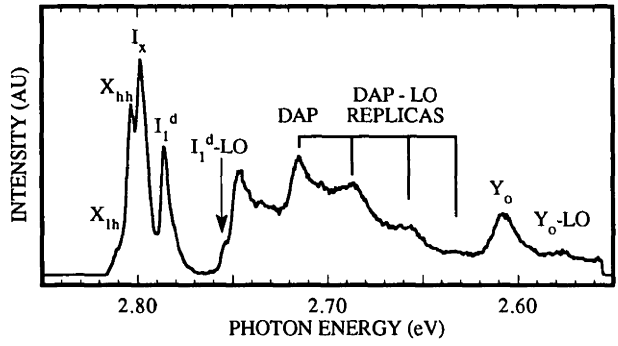

Figure 6. Photoluminescence spectrum at T = 9 K for an undoped 230 nm-thick ZnSe film grown on (001) GaAs by PLA.

ACKNOWLEDGEMENT

This research was sponsored by the Division of Materials Sciences, U.S. Department of Energy under contract DE-AC05-84OR21400 with Martin Marietta Energy Systems, Inc..

REFERENCES

1. B. S. Wherrett, *Semicond. Sci.Tech.* **6**, A65 (1991).
2. *From Optical Bistability Towards Optical Computing*, edited by P. Mandel, S. D. Smith, B. S. Wherrett, North-Holland, New York, 1987.
3. W. J. Walecki, A. V. Nurmikko, N. Samarth, H. Luo, J. K. Furdyna, *J. Opt. Soc. Am. B* **8**, 1799 (1991).
4. T. Saitoh, T. Yokogawa, T. Narusawa, *Jpn. J. Appl. Phys.* **30**, 667 (1991).
5. S. Yamaga, *Jpn. J. Appl. Phys.* **30**, 437 (1991).
6. M. A. Haase, J. Qiu, J. M. DePuydt, H. Cheng, *Appl. Phys. Lett.* **59**, 1272 (1991).
7. J. T. Cheung, H. Sankur, *CRC Critical Reviews in Solid State and Materials Sciences*, **15**, 63 (1988).
8. J. J. Dubowski, J. R. Thompson, S. J. Rolfe, J. P. McCaffrey, *Superlattices and Micorstructures* **9**, 327 (1991).
9. J. W. McCamy, D. H. Lowndes, J. D. Budai, B. C. Chakoumakos, R. A. Zuhr, "Growth of Epitaxial ZnS Films by Pulsed-Laser Ablation," in *Wide Band-Gap Semiconductors*, (Mater. Res. Soc.**24**, Pittsburgh, PA, 1992).
10. J. W. McCamy, D. H. Lowndes, J. D. Budai, in *1992 International Conference on Solid State Devices and Materials*, Tsukuba, Japan, 1992, pp. 357–359.
11. N. T. Pelekanos, J. Ding, M. Hargerott, A. V. Nurmikko, H. Luo, N. Samarth, J. K. Furdyna, *Phys. Rev. B* **45**, 6037 (1992).
12. N. Samarth, H. Luo, J. K. Furdyna, R. G. Alonso, Y. R. Lee, A. K. Ramdas, S. B. Qadri, N. Otsuka, *Appl. Phys. Lett*. **56**, 1163 (1990).
13. G. E. Jellison, Jr., F. A. Modine, *Appl. Opt.* **29**, 959 (1990).
14. G. E. Jellison, Jr., J. W. McCamy, *Appl. Phys. Lett.* **60**, 512 (1992).
15. D. Bertho, D. Boiron, A. Simon, C. Jouanin, C. Priester, *Phys. Rev. B* **44**, 6118 (1991).
16. Y. Wu, K. Ichino, Y. Kawakami, S. Fujita, S. Fujita, *Jpn. J. Appl. Phys.***31**, 1737 (1992).
17. J. P. Walter, M. L. Cohen, *Phys. Rev.* **183**, 763 (1969).
18. S. Adachi, T. Taguchi, *Phys. Rev. B* **43**, 9569 (1991).
19. T. Yao, "MBE of II-VI Compounds" in *The Technology and Physics of Molecular Beam Epitaxy*, edited by E. H. C. Parker, Plenum Press, New York, 1985.